

Recent Progress of High Power Semiconductor Lasers for EDFA Pumping

by Akihiko Kasukawa*, Toshikazu Mukaihara*, Takeharu Yamaguchi* and Jun'jiro Kikawa*

ABSTRACT Optical fiber communication systems using a WDM (wavelength division multiplexing) system are being introduced in long-haul networks to manage the explosive increase in transmission capacity. Erbium-doped fiber amplifier (EDFA) is one of the key components to support WDM systems. High power lasers emitting at both 980 nm and 1480 nm are essential for pumping sources for EDFA. In this paper, state-of-the-art high power pumping lasers are reviewed. Furukawa Electric has succeeded to release high performance and high reliable pumping lasers. In particular, ultra-high output power of 250 mW-1480 nm modules have been commercialized. These high output power laser modules are of great importance for Raman amplifiers as well as EDFA applications.

1. INTRODUCTION

Optical fiber communication systems have realized large transmission capacity; however, bit rate increase utilizing traditional TDM (time division multiplexing) cannot manage the explosive demands for larger transmission capacity triggered by data communication and Internet. The urgent demands for larger transmission capacity have driven system planners to introduce WDM systems instead of TDM systems to make the best use of installed optical fibers.

WDM systems are thought to be the most cost-effective way to handle the increasing transmission capacity using established transmission technologies. In WDM systems, which use multi-channel single frequency lasers such as distributed feedback lasers with slightly different wavelengths determined by ITU (International Telecommunication Union), total throughput transmission capacity can be increased by the number of lasers (channels).

Transmission capacity trends are illustrated in Figure 1 for both commercial implementations and laboratory demonstrations. Total transmission capacity of more than 100 Gbps can be easily realized by using the established 2.5-Gbps and developing 10-Gbps technology. Extremely large transmission capacity of more than 1 Tbps will be realized in the near future utilizing WDM systems.

On the other hand, strict specifications are required for optical devices in terms of wavelength, since WDM systems utilize the wavelength regime. Single frequency lasers used in the systems, for example, have to control the absolute lasing wavelength to meet the ITU grid as well as wavelength separation. The wavelength separa-

tion according to ITU, for example, is set to be 1.6 nm (200 GHz), 0.8 nm (100 GHz) and 0.4 nm (50 GHz) depending on the WDM channels (bit rate).

In addition to the strict requirements in wavelength control, signal light sources have to have high output power in order not only to extend the transmission distance but to compensate for the insertion loss caused by the many optical components like the wavelength coupler used in WDM systems.

In order to amplify the signal light source in an efficient way, optical amplifiers are the key component to support WDM systems. Erbium-doped fiber amplifiers (EDFAs), which will be described later, have an advantage over traditional O/E and E/O amplification because of the excellent amplification characteristics such as high speed, simultaneous amplification of many channels and so forth.

Higher pumping power can make it possible to produce higher signal output power. Therefore, high power semiconductor lasers are one of the key devices for pumping erbium-doped fibers (EDFs).

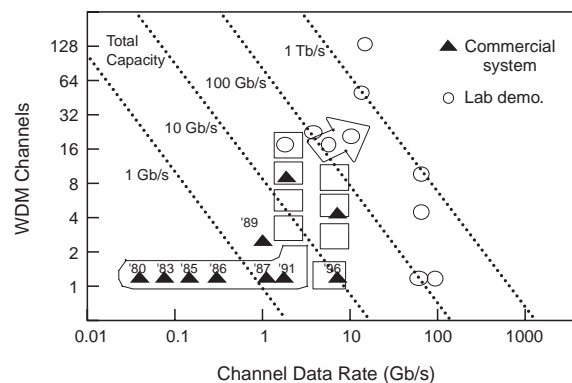


Figure 1 Progress of transmission systems speed based on WDM

* Semiconductor R&D Center, Yokohama R&D Laboratories

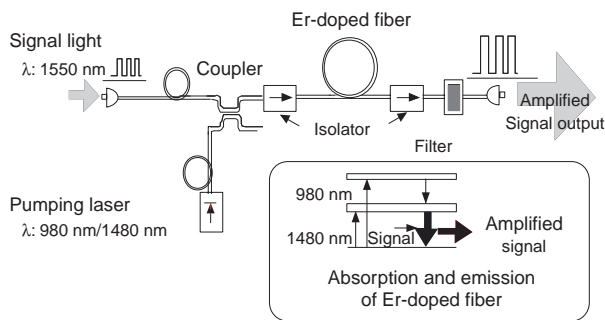


Figure 2 Configuration of optical fiber amplifier

2. OPTICAL FIBER AMPLIFIER (OFA)

It is no exaggeration to say that the invention of the optical fiber amplifier is the innovation making it possible to realize the WDM system. In particular, the EDFA¹⁾ is very attractive for practical application because light amplification occurs in the wavelength range of the 1500-nm band, which is the low loss wavelength region of conventional silica fibers.

Figure 2 illustrates the configuration of EDFA. It consists of EDF, a pumping laser module, a WDM coupler to couple the pumping light into EDF, an optical isolator to prevent the lasing in the EDF, and an optical fiber.

High power lasers emitting at wavelengths of 980 nm and 1480 nm are used as pumping sources for effective pumping of EDF. Efficient power conversion can be realized with a 1480-nm pump²⁾, while low noise amplification can be realized with a 980-nm pump. In practical application, 1480-nm pumping is used as a booster amplifier and 980-nm pumping is used as a pre-amplifier.

3. SEMICONDUCTOR MATERIAL AND EPI-TAXIAL GROWTH

1480-nm lasers can be fabricated using the conventional GaInAsP quaternary compound on an InP substrate, which has been used for telecommunication lasers emitting at 1300 nm and 1550 nm. We can use the established technology. On the other hand, 980-nm lasers cannot be fabricated by use of lattice matched materials. The wavelength of around 980 nm emitted from semiconductor lasers has been a forbidden wavelength region which cannot be covered by traditional short wavelength GaAs-based lasers (wavelength of shorter than 900 nm) and InP-based long wavelength lasers (wavelength longer than 1200 nm). The concept of strained-layer quantum wells^{3), 4)}, however, made it possible to realize 980-nm lasers as well as rapid progress of epitaxial growth technique to grow high quality very thin strained-layer material. 980-nm lasers can be fabricated by use of an intentionally lattice-mismatched In_xGaAs layer on a GaAs substrate. The In_xGaAs strained-layer has a large lattice constant with respect to GaAs. If the layer thickness is controlled within the critical thickness calculated by Mathew's law, the layer can be grown with high crystalline quality on a

GaAs substrate even if the InGaAs layer has a large amount of strain. This condition is approximately given by $\varepsilon L_z < 20 \text{ nm}\%$ ⁵⁾, where ε is the amount of strain and L_z is the layer thickness.

Strained-layer GaInAsP on an InP substrate is also used for 1480-nm lasers since the concept of strained-layer quantum can improve the lasing characteristics drastically.

Let's explain the quantum wells and strained-layer quantum wells used in high performance 980-nm and 1480-nm lasers. Quantum wells are made up of two different materials with a layer thickness less than the de Broglie wavelength, say 20 nm. High material gain can be obtained with less carriers because carriers are effectively confined to the quantized state formed by the quantum well. In particular, the use of compressive strain into the quantum wells can change the modification of valence band structure in such a way that the effective mass of heavy-hole becomes light. As a result, the Bernard-Duraffourg condition (Fermi-level separation larger than energy band-gap) can be satisfied with less carrier density. Thus, lower threshold current density and higher quantum efficiency can be obtained in strained-layer quantum well lasers.

A strained-layer quantum well laser wafer can be grown by metalorganic chemical vapor deposition (MOCVD) for both 980 nm and 1480 nm.

4. APPROACH FOR HIGH POWER OPERATION

In a practical application, a laser diode module, so-called pig tailed module, is used. The laser diode has to be designed in such a way that high power operation is obtained with a narrow and circular beam for high coupling into a single mode fiber (SMF). It should be noted that highly reliable operation under high output power has to be realized. For these purposes, buried heterostructure (BH) structure is used for 1480-nm lasers and a ridge waveguide (RWG) structure is used for 980-nm lasers.

The limiting factors for high power operation under a continuous wave (CW) condition in these narrow stripe lasers are categorized into two phenomena; one is roll-over phenomenon due to the increase of temperature in the active layer or increase of invalid current, and the other is catastrophic phenomenon mainly due to the optical mirror damage. The former is observed in 1480-nm lasers, and the latter is the sudden death phenomenon called catastrophic optical mirror damage (COD) and is observed mainly in 980-nm lasers. A detailed explanation of the COD is reported in reference 6.

Let's explain the approach of how to attain high power operation in solitary lasers. The output power from the front facet, P_f is given by the following equation if COD does not occur.

$$P_f = \eta_i \frac{1}{1 + \frac{1-R_f}{1-R_r} \sqrt{\frac{R_r}{R_f}}} \times \frac{\alpha_m}{\alpha_i + \alpha_m} (I - I_{th}) \left(\frac{I_{ac}}{I_{ac} + I_L} \right) \Theta(T)$$

Where, η_i : internal quantum efficiency, α_i : internal loss, α_m : mirror loss, I : injection current, I_{th} : threshold current, I_{ac} : effective current which contributes to the lasing, I_L : leakage current, and $\Theta(T)$: term representing the optical power output saturation due to heat generation.

From this equation, the following measures are thought to be effective for high power operation.

- (a) realization of high internal efficiency
- (b) introduction of asymmetric coating for low mirror loss
- (c) realization of low internal loss
- (d) suppression of leakage current
- (e) high thermal dissipation

Structural optimizations have to be made because contradictory items are included in the above. The introduction of a long cavity, for example, is effective for low thermal resistance, however, increase of the threshold current and decrease of external quantum efficiency are observed in long cavity lasers.

Detailed explanations for realizing the above items are given as follows.

(a) In order to achieve high internal quantum efficiency, structures of both quantum wells and optical confinement layers such as composition and thickness have to be optimized carefully. Introduction of strained layer quantum wells into the active layer is indispensable for this purpose. The use of GRIN-SCH (Graded-Index Separate-Confinement-Structure) is very effective⁷⁾ for high internal quantum efficiency, which will be described in detail later.

(b) Parallel mirror formed by cleavage of semiconductor material is used for Fabry-Perot resonator, thus, an equal amount of light is emitted from both sides of the mirror. The output power from the rear facet is not so important because it is used only for a back-monitor in a practical application. Therefore, asymmetric facet coatings composed of dielectric mirror are used to increase the output power from the front facet. Low reflective coating (several percent) is used for the front facet and high reflective coating (95%) is used for the rear facet.

(c) Introduction of quantum well structure, especially a strained-layer quantum well is effective for low internal loss. A strained-layer quantum well laser can provide low threshold current and high differential quantum efficiency operation due to low internal loss even if a long cavity is used.

(d) The reduction of leakage current leads to the suppression of temperature rise of the active layer, thus leading to the high power operation.

(e) It is possible to reduce the temperature rise in the active layer by the use of a long cavity (low electric and thermal resistance) and junction down bonding on heat sink materials with high thermal conductivity such as diamond and AlN.

Next, the output beam design for achieving high coupling into an SMF is explained. High coupling efficiency into an SMF is indispensable for fabricating a high power

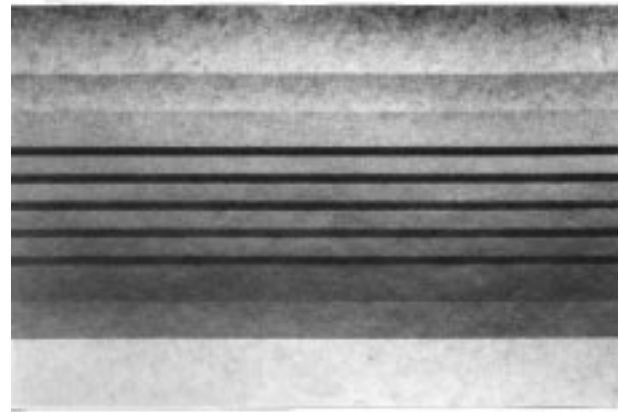


Figure 3 TEM image of the active region of a 1480-nm laser

laser diode module. Narrow and circular output beams are favorable for efficient fiber coupling. Output beam characteristics can be controlled by the layer composition and thickness of the GaInAsP layer⁷⁾ which form the SCH layer. In particular, the use of a GRIN-SCH layer can expand design freedom by not only taking into account the carrier confinement into the active layer but also optical confinement as well. It is theoretically and experimentally verified that the use of a GRIN-SCH layer comprising a thinner and wider bandgap is effective for both output beam characteristics and low threshold current, high quantum efficiency operations.

It is noted that the packaging design, including coupling lens system, is also very important for high coupling efficiency into an SMF.

5. CHARACTERISTICS OF 1480 NM LASERS

Transmission electron microscopy of a cross sectional view of the active layer for a 1480-nm laser is shown in Figure 3. The active layer is made up of 1% compressively strained quantum wells (4 nm thick) separated by GaInAsP (10 nm thick) with a bandgap wavelength of 1.2 μm . The number of wells is five. The GRIN-SCH layer, composed of two different GaInAsP, sandwiches the strained-layer active layer. The use of GRIN-SCH structure is shown to be effective for high performance in the long wavelength region⁹⁾. Very sharp hetero-interfaces are obtained through MOCVD growth optimization.

BH structure with an active layer width of 2 μm is used for both electrical and optical confinements. All epitaxial growth, including selective growth for BH structure using MOCVD process, ensures a high yield process using a 2-inch wafer.

Figure 4 shows the injection current versus light output power characteristics for an optimized 1480-nm laser. The cavity length is 1200 μm for high heat dissipation, which is longer than those of conventional lasers having typical cavity lengths of 300-400 μm used for telecommunication applications. In order to increase the heat dissipation, the

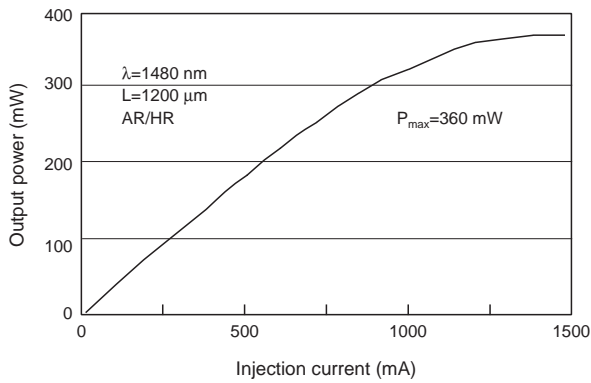


Figure 4 I-L characteristics of 1480-nm laser

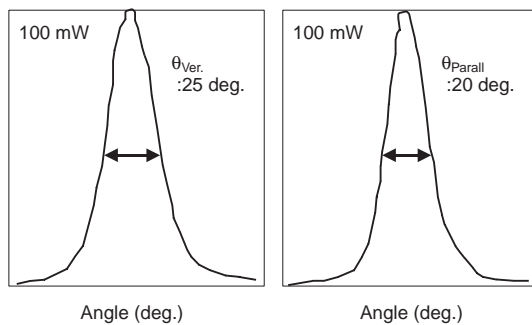


Figure 5 Output beam pattern of 1480-nm laser

laser is bonded with a junction down configuration, that is, the laser is bonded on a heat sink in such a way that the active layer, which is the main heat generator, lies close to the heat sink. The facet is coated with an AR/HR film. The reflectivities are 5% and 95% for front and rear facets, respectively. Low threshold current of 25 mA was obtained in spite of a long cavity of 1200 μm . Output power as high as 360 mW from the front facet was achieved, which, to the best of our knowledge, is the maximum output power ever reported for transverse-mode stabilized long wavelength lasers⁷⁾. High output power of over 300 mW was obtained even at a high temperature of 50°C. Extremely high output power was obtained for this particular device with a long cavity, however, driving current or power consumption is relatively high for 100-200 mW output power, which is commonly used for practical application. Therefore, a cavity length around 800-1000 μm is used for low power consumption operation. Maximum output power is decreased due to the poor heat dissipation, however, driving current for 100-200 mW can be decreased because of higher differential quantum efficiency.

Figure 5 shows the far field pattern (FFP) parallel and perpendicular to the junction plane at an output power of 100 mW. Full-width at half-maximums of FFP parallel and perpendicular to the junction plane are 20° and 25°, respectively. The narrow and circular output beam obtained here is favorable for high coupling into SMF.

Highly reliable operation must be achieved like conventional FP and DFB lasers since optical fiber amplifiers are used for long-haul trunk lines and submarine optical com-

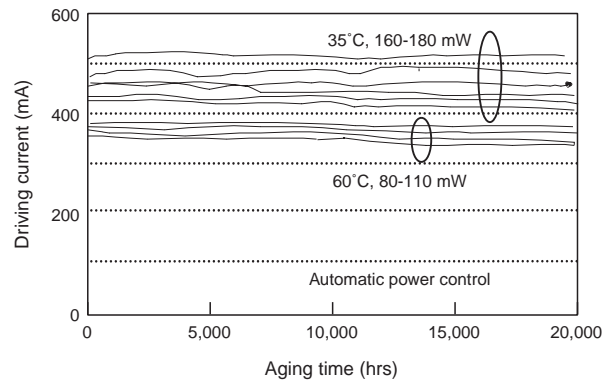


Figure 6 Reliability test results of 1480-nm laser

munication systems. Output power of pumping lasers is extremely high as compared to conventional signal lasers. Reliability test under high temperature and high output power has to be investigated. Figure 6 shows the aging test result at high power condition. The aging test has been performed at 35°C and 60°C in the automatic power control mode. The output power is set to be 80% of the maximum output power at a given temperature, determined by the thermal roll-over, which is 180 mW at 35°C and 120 mW at 60°C. Stable operation has been confirmed after 20000 hours without appreciable increase of driving current. The activation energy of 0.62 eV is derived from various aging test conditions. Extremely high reliability of 100 million hours as a mean time to failure (MTTF) is estimated at an output power of 150 mW, which corresponds to the module output power of 120 mW (reasonable coupling efficiency into an SMF of 80% is assumed).

6. CHARACTERISTICS OF 980-NM LASERS

The noise figure of fiber amplifiers pumped at 980 nm is lower than that of fiber amplifiers pumped at 1480 nm, which is very attractive for practical application.

The material candidate for 980-nm lasers is compressively strained InGaAs quantum wells for the active layer, while there are two candidates for cladding layer materials. Those are conventional AlGaAs¹⁰⁾⁻¹⁴⁾ layer and novel InGaP^{15), 16)} layers. The use of InGaP cladding layer material might have an advantage over AlGaAs in terms of less oxidized property and slow surface recombination velocity, which are thought to be effective methods to suppress COD.

As mentioned previously, transverse-mode stabilized laser structure is used for efficient coupling to SMF. Ridge waveguide structure is widely used as shown in Figure 7. This laser structure is grown by MOCVD. Recently, other laser structures like buried ridge waveguide structure and self-aligned-structure (SAS) have been investigated.

Light output power versus injection current characteristics is shown in Figure 8 for a 980-nm RWG laser with 4 μm -wide ridge and 800 μm -long cavity. Light output power

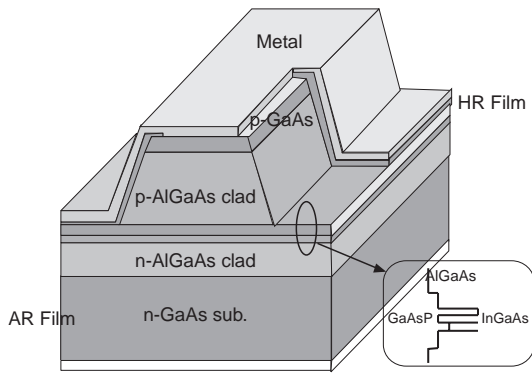


Figure 7 Structure of ridge-waveguide type 980-nm laser

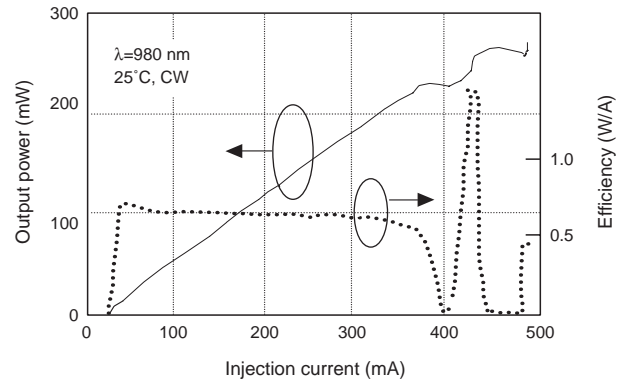


Figure 10 I-L characteristics of 980-nm laser module

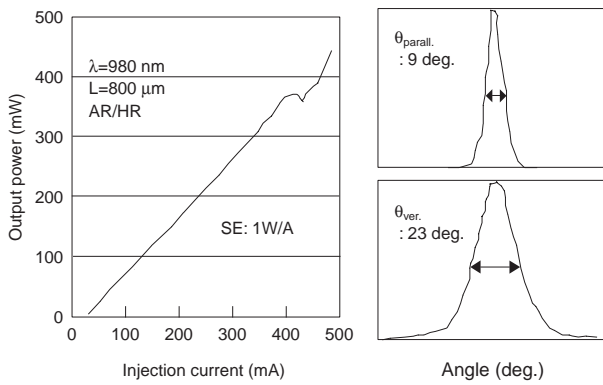


Figure 8 I-L characteristics of 980-nm laser

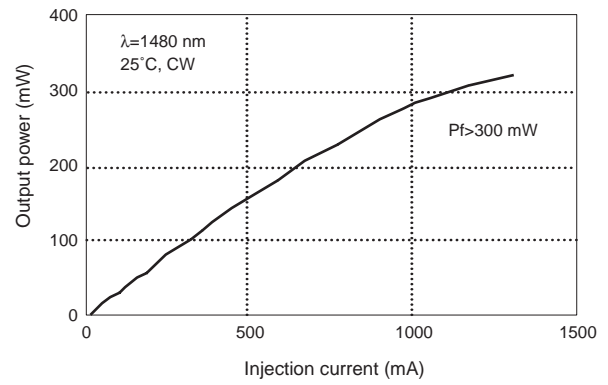


Figure 11 I-L characteristics of 1480-nm laser module

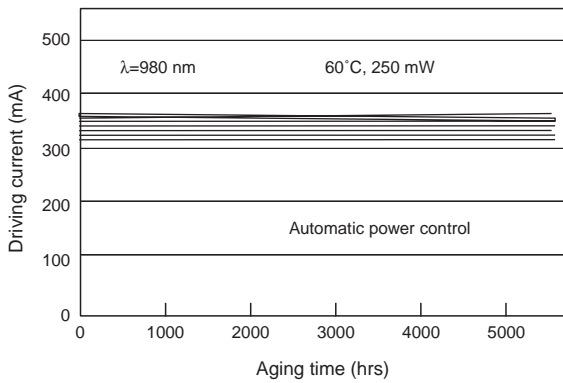


Figure 9 Reliability test results of 980-nm laser

more than 300 mW was successfully achieved with a slope efficiency as high as 1 W/A. FFPs parallel and perpendicular to the junction plane are also shown in Figure 8 at an output power of 250 mW, showing an elliptical output beam as compared to BH lasers. It is possible to obtain high coupling efficiency by optimizing a coupling scheme. With a wedge-shaped fiber, which is specially designed for beam shape, coupling efficiency as high as 80% was achieved.

Similar to 1480-nm lasers, highly reliable operation is required. One of the key items for high reliability operation is to overcome COD. Key technology is facet passivation technology. Several approaches have been reported, those are, cleavage laser bars in the ultra-high-vacuum

atmosphere and in-situ facet passivation, facet passivation using high thermal conductivity material, and formation of so-called 'window structure' near the facet, which is transparent to the emission wavelength.

Long term aging result is shown in Figure 9 under conditions of 60°C, 250 mW. No appreciable change in driving current has been observed after 5000 hours.

7. LASER MODULE

Figures 10 and 11 show the light output power versus injection current characteristics of 980-nm and 1480-nm laser modules, respectively. Very high coupled powers of 200 mW for a 980-nm laser module¹⁷⁾ and of over 300 mW for a 1480-nm laser module¹⁸⁾ are obtained.

In particular, coupled power of over 300 mW is the highest power reported for long wavelength laser modules with SMF. Extremely high coupled power modules of 250 mW are commercially available.

The failure mode related to the packaging has been reported in 980-nm laser modules. It is considered that hydrocarbon, contained in epoxy used for package and adhering to the laser facet is the trigger for COD. This failure mode is called PIF (package induced failure). One solution to avoid PIF is to introduce a small amount of oxygen into the package to burn out the hydrocarbon adhered to the laser facet.

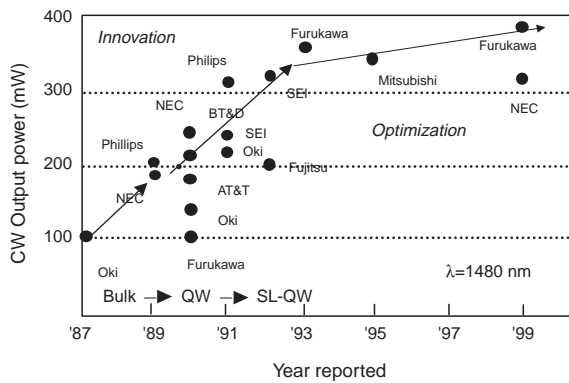


Figure 12 Improvements in light output of 1480-nm laser

Several types of laser modules have been fabricated for WDM application. Wavelength stabilized laser module is one example¹⁹⁾. Lasing wavelength can be stabilized by the use of fiber Bragg grating. In general, lasing wavelength of FP lasers shifts to longer wavelengths with a temperature coefficient of 0.5 nm/degree in the 1480-nm wavelength. By using fiber Bragg grating with a narrow pass band, a stable lasing wavelength for both current and temperature can be achieved.

8. FUTURE PROSPECT

The history for power improvement in narrow stripe (transverse-mode stabilized) 1480-nm lasers is shown in Figure 12. Drastic power improvement has been achieved by technological innovations, such as, introduction of quantum well active layer and strained-layer quantum well active layer. By using a strained-layer quantum well active layer, maximum output power of about 400 mW was

achieved. New technological innovations such as a novel active layer structure and some consideration for active layer material can lead to further output power improvement in the future.

ACKNOWLEDGEMENT

The authors would like to thank Drs. K. Ohkubo, Y. Suzuki, T. Kamiya for their encouragement and also the entire pump laser team including FITEL products division.

REFERENCES

- 1) S. B. Poole et al: Electron. Lett., 21 (1985) 737.
- 2) K. Nishimura : Optical soliton transmission Technical Report , 1995, p.57. (in Japanese)
- 3) E. Yablonovitch at al: J. Lightwave Technol., LT-4 (1986) 504.
- 4) A. R. Adams: Electron. Lett., 22 (1986) 249.
- 5) T. J. Andersson et al.: Appl. Phys. Lett., 51 (1987) 752.
- 6) I. Mito et al.: Applied Physics Japan, 64 (1995) 2. (in Japanese)
- 7) A. Kasukawa et al.: IEEE Photon. Technol. Lett., 1 (1994) 4.
- 8) A. Kasukawa et al.: OPTOELECTRONICS-Device and Technologies, 9 (1994) 219.
- 9) H. Hirayama et al.: IEEE J. Quantum Electron., 28 (1992) 68.
- 10) D. Fekete et al.: Appl. Phys. Lett., 49 (1986) 1659.
- 11) M. Okayasu et al.: IEEE Photon. Technol. Lett., 2 (1990) 689.
- 12) S. Ishikawa et al.: IEEE J. Quantum Electron., 29 (1993) 1936.
- 13) H. Meier: Technical Digest of 20th European Conference on Optical Communications, Firenze, Sep., 1994, p.974.
- 14) J. S. Major et al.: Electron. Lett., 27 (1991) 540.
- 15) S. Sagawa et al.: Technical Digest of 14th International Semiconductor Laser Conference, Maui, Sep., 1994, p.255.
- 16) M. Ohkubo et al.: IEEE J. Quantum Electron., 30 (1994) 1936.
- 17) Y. Irie et al.: OFC/IOOC'99, Paper WM15 (1999).
- 18) T. Kimura et al.: OAA'99, Paper ThD12 (1999).
- 19) S. Koyanagi et al.: OAA'98, p.35 (1998).

Manuscript received on December 17, 1999.